Regional patterns of hydroclimate variability in southeastern Australia over the past 1200 years

Bronwyn C. Dixon[1], Jonathan J. Tyler[2], Benjamin J. Henley[3,4,5,6], Russell N. Drysdale[1,7]

[1]School of Geography, University of Melbourne, Parkville, 3010, Australia.

[2]Department of Earth Sciences and Sprigg Geobiology Centre, University of Adelaide, Adelaide, 5005, Australia.

[3]School of Earth Sciences, University of Melbourne, Parkville, 3010, Australia.

[4]ARC Centre of Excellence for Climate Extremes, University of Melbourne, Parkville, 3010, Australia.

[5]School of Earth, Atmosphere and Environment, Monash University, Clayton, 3168, Australia.

[6]Infrastructure Engineering, University of Melbourne, Parkville, 3010, Australia.

[7]Laboratoire EDYTEM UMR CNRS 5204, Université Savoie Mont Blanc, 73376 Le Bourget du Lac, France

Corresponding author: Bronwyn C. Dixon (bdixon1@student.unimelb.edu.au)

Key Points:

- Southeastern Australia experienced cooler and wetter conditions during the Little Ice Age, with increased winter rainfall.
- Temperature may have played a role in controlling effective moisture in the region during the last 1200 years by decreasing evaporation.
- Australian decadally and annually resolved palaeoclimate archives show similar low-frequency patterns during the Common Era, although the signal in the latter is more attenuated.

Plain language summary

Changes in the characteristics of natural materials, such as ice, trees, and lake mud, allows us to know how the climate has changed in the past. This is particularly important in Australia, where climate varies drastically but written climate records go back less than 100 years. In this study, we look at these changes in natural materials at eight locations across southeastern Australia. Although each location has its own history, we find common patterns between all the sites. Southeast Australia has generally gotten rainier between 1050 years ago and 200 years ago. Temperatures were cooler at the same time, so the rain could nourish the landscape more rather than just drying out immediately. The rainiest time happened 550-350 years ago, when most of the rain was coming up from the Southern Ocean during winter. Finding these common patterns in natural sources from different locations makes us more certain about how the climate has changed in the past and can help us to know how the climate may change into the future.

Abstract

Long, continuous palaeoclimate records provide an opportunity to extend knowledge of decadal to multi-decadal scale climate variability beyond the limit of instrumental records. In this study, quality-controlled proxy records from southeastern Australia are examined for coherent variability during the Common Era, with age uncertainty for each record estimated using iterative age modeling. Site-level empirical orthogonal functions (EOFs) are derived from multivariate records for the purpose of objective comparison of climate signals between sites without selection bias. A regional Monte Carlo EOF (MCEOF) analysis is conducted on combined time-uncertain single-proxy records and site-level EOFs. The analysis identifies two robust vectors, which are inferred to represent hydroclimate changes. The first regional MCEOF suggests an increase in effective moisture between 900 – 1750 CE. Agreement between regional MCEOF1 and Australian temperature reconstructions suggests suppressed evaporation was a significant influence on regional effective moisture during this time. Regional MCEOF2 exhibits shorter, centennial-scale oscillations that show some similarity with rainfall reconstructions based on remote high-resolution proxies. We interpret MCEOF2 to represent regional-scale rainfall patterns driven by changes in seasonal rainfall and the influence of the Southern Annular Mode over southern Australian rainfall. This study presents the first quantitative regional synthesis of southeastern Australian hydroclimate reconstructions from multivariate sedimentary

archives covering the last 1200 years. The resulting MCEOFs demonstrate the utility of low-resolution climate records from this region, but also highlight the limitations of the existing data network, which must be resolved through the generation of new records.

1 Introduction

Recent decades have been characterized by periods of severe drought and seasonal rainfall decreases across parts of the Australian continent (Gergis et al., 2012; Taschetto & England, 2009; van Dijk et al., 2013). However, the drivers of these apparently extreme events in the context of longer-term hydroclimate variability remain unclear, especially on decadal to multi-decadal time scales (Cai et al., 2014; Kiem et al., 2016; van Dijk et al., 2013). Instrumental observations in Australia extend back to the late 1800s at most, but many studies examining climate variability use datasets covering only part of the 20th century (Ansell et al., 2000; Kiem & Franks, 2004; Kiem et al., 2003). This provides only a short reference period for examining the causes of rainfall variability on multi-decadal time scales (Ashcroft et al., 2014; Gallant et al., 2011). Additionally, climate-model projections for Australia have suggested that drying trends in southern Australia will continue, along with an intensification of drought frequency and duration (Grose et al., 2015). These projections can be placed into a broader context through comparison with sufficiently long paleoclimate baselines.

Australian climate is strongly impacted by the interaction of coupled ocean-atmosphere climate modes (i.e. the El Niño-Southern Oscillation (ENSO), and the Indian Ocean Dipole (IOD)) because of the continent's location at the intersection of the Indian and Pacific Oceans (Ashok et al., 2003; Power et al., 1999a; Power et al., 1999b). Decadal variability of interannual modes and their impacts is pronounced, particularly in the Pacific (Power et al. 1999; Henley et al. 2015). Coupled modes and hemispheric atmospheric circulation patterns (i.e. the Southern Annular Mode (SAM) (Hendon et al., 2007)) control the origin and amount of regional precipitation (Risbey et al., 2009). Interaction of these modes explains much of the decadal variability in southeastern Australian rainfall during the 20th century (Murphy & Timbal, 2008; Speer et al., 2011); however, only a few proxy-based studies have attempted to extend this knowledge beyond the instrumental period (Allen et al., 2017; Allen et al., 2015; Freund et al., 2017; Palmer et al., 2015). Model-based future projections rely on the skill and reliability of models to characterize key ocean-atmosphere processes. However, the latest generation of climate models

varies widely in their ability to capture the observed spatial and temporal behavior of modes of variability (Bellenger et al., 2014; Henley et al., 2017; Weller & Cai, 2013; Zheng et al., 2013).

Proxy-based paleoclimate records have a unique potential to complement instrumental and model data and provide a critical longer-term reference for observed changes and variability (Gallant et al., 2011; Henley et al., 2011; Neukom & Gergis, 2012; Treble et al., 2003). The Common Era, the period of the last ~2000 years, is adopted widely as an appropriate reference for placing recent (the last ~200 years) climate fluctuations into the context of natural variability under the current boundary conditions (PAGES2k Consortium, 2013, Dixon et al., 2017).

Efforts to reconstruct multi-decadal scale climate variability and examine possible influences of climate drivers on decadal precipitation in the Australasian region have primarily relied on annually resolved paleoclimate archives, such as tree rings, corals, and ice cores (Cook et al., 2006; Cullen & Grierson, 2009; Gergis et al., 2016; Hendy et al., 2002; Lough, 2007; van Ommen & Morgan, 2010; T. R. Vance et al., 2013). The geographic distribution of these multi-century paleoclimate reconstructions is restricted mostly to tropical coastal regions and mountainous regions of Tasmania (Neukom & Gergis, 2012), which presents a significant challenge for examining the influences of climate variability across most of mainland Australia. Long, continuously sampled sedimentary records can provide multi-decadal to millennial-scale paleoclimate reconstructions where annually resolved records are scarce. These sedimentary records present challenges in the form of variable time resolution and dating uncertainty, but these limitations can be acknowledged and incorporated into data syntheses and interpretations (Anchukaitis & Tierney, 2012; Tyler et al., 2015). The Australasian region has over 600 non-annually resolved (lower resolution) sedimentary archives covering the late Holocene. These records were recently identified and systematically assessed for their suitability for inclusion in a regional, multi-centennial hydroclimate reconstruction, a process which identified 22 records, eight of which are in south-eastern Australia (Dixon et al., 2017a). The hydroclimate datasets identified by Dixon et al. (2017) represent a diverse suite of environments and measured proxies, each of which may subtly respond differently to climate. Geomorphological, geochemical, and ecological differences inherent in paleoclimate archives influence the preservation of climate signals (Battarbee, 2000; Fairchild et al., 2006; Fritz, 2008; Mason et al., 1994; Wigdahl et al., 2014). However, identification of common signals across multiple sites offers the potential to identify broad climate-driven signals and overcome archive-specific idiosyncrasies.

Reconstructions from long, continuous sedimentary paleoclimate records provide a means for independently evaluating the integrity of multidecadal to centennial variability captured by annually and sub-annually resolved paleoclimate records in Australia.

Empirical Orthogonal Function (EOF) analysis is a commonly applied technique in climate and paleoclimate research, having been successfully used to identify climate signals across data networks at differing temporal and spatial scales. EOFs have been used with tree ring reconstructions to identify and characterize common climate signals within regional compilations of annual chronologies (Buckley et al., 2000; Cook et al., 2000; Cook et al., 2006; Palmer et al., 2015), as well as identifying common signals across multiple tree species (Andreu et al., 2007). Clark et al. (2007) and Shakun and Carlson (2010) employed EOF analysis with a global paleoclimate data network to investigate the spatial and temporal consistency of peak glacial conditions during the last glacial cycle. Anchukaitis and Tierney (2012) incorporated chronological uncertainty into an EOF approach using seven sedimentary records covering the late Holocene in southeastern Africa. Their research identified the dominant influence of the Indian Ocean over southeastern Africa during the Common Era (Tierney et al., 2013). Tyler et al. (2015) further explored the potential to apply multi-tiered ordination to identify common signals both within, and between, multivariate paleoclimate datasets. Common modes of variability between diatom assemblages in the sediments of four Australian lakes were inferred to reflect ecological change influenced by regional hydroclimate conditions. The timing and strength of response varied by lake basin, but there was a general pattern of increased moisture between approximately 500 and 200 yr BP. This study builds upon the approach taken by Tyler et al. (2015) by expanding the spatial coverage of records to a greater area of southeastern Australia, incorporating a diversity of archives, and assessing the efficacy of performing data reduction on multivariate sedimentary records.

The aims of this paper are: i) to derive a new, more robust regional hydroclimate reconstruction for southeastern Australia based on multi-decadal paleoclimate records from a diverse collection of collection archives ii) to assess the efficacy of single- versus multi-tiered data reduction approaches for synthesizing southeastern Australian paleoclimate data; and iii) to critically compare the new reconstruction to existing multi-centennial regional and hemispheric paleoclimate records. A comparison between annually and non-annually resolved multi-

centennial paleoclimate reconstructions may help to clarify the impact of resolution and archive type on the preservation of low-frequency climate signals.

2 Methods

2.1 Data

A recent study evaluated a comprehensive metadatabase of 675 Australasian paleoclimate records that span all or a portion of the last 2000 years. Twenty-two records were identified as meeting stringent criteria for suitability to investigate decadal to centennial climate variability during the Common Era (Dixon et al., 2017a). Those selection criteria were: i) the proxy must have an identified relation with one or more climate variables, as stated in a peer-reviewed publication; ii) the record must extend continuously for at least 500 out of the last 2000 years; iii) the record must have an age model based on at least two chronological anchors; iv) the record must have an average sample resolution between 2-50 years per sample; and v) the collection location must fall within the Australasian climate region (90°E - 140°W, 10°N - 80°S) (Gergis et al., 2016). These criteria were established by the International Geosphere-Biosphere Program's Past Global Changes (PAGES) 'Regional 2k' initiative (PAGES2k Consortium; Dixon et al., 2017).

Eight of the records that met the selection criteria represent hydroclimate variability and are located within southeastern Australia (Dixon et al., 2017; Figure 1, Table 1). These records provide a unique opportunity to identify spatial and temporal patterns across a region for which multi-centennial paleoclimate records are scarce. All of the records are previously published and are archived at the NOAA paleoclimate archive (https://www.ncdc.noaa.gov/data-access/paleoclimatology-data/datasets). The hydroclimate reconstructions mostly represent input/evaporation balance (I/E), where input may include direct precipitation, groundwater inflow, through-flow, and/or surface runoff.

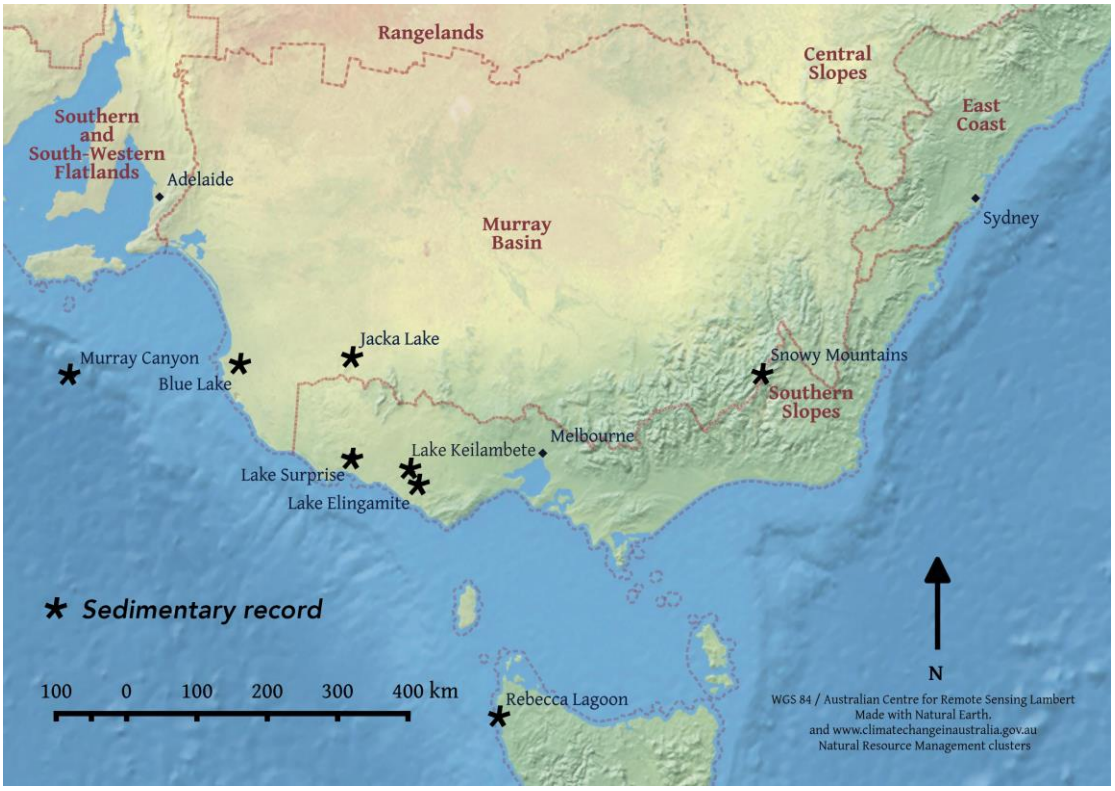

Figure 1. The locations of existing southeastern Australian hydroclimate reconstructions, as identified by Dixon et al., 2017. The boundaries of Natural Resource Management (NRM) regions are shown with a maroon outline.

Table 1. Metadata for southeastern Australian sedimentary hydroclimate records, including record name, state where record was collected (SA=South Australia, VIC=Victoria, TAS=Tasmania, NSW=New South Wales), latitude, longitude, elevation (meters above sea level), archive, measured proxies, climate variable as interpreted by the original authors (SST=sea surface temperature, I/E = Input/evaporation ratio), original reference, average record resolution, and data archive URL.

Record Name	State	Latitude	Longitude	Elevation (m)	Archive	Proxy	Interpreted Climate Variable	Original Reference	Average Temporal Resolution (years)	Archive URL
Murray Canyon	SA	-37.26	137.36	-2420	Foraminifera	δ18O, ecological assemblage	SST, ENSO activity	Moros et al. (2009a); Moros et al. (2009b)	40	https://www.ncdc.noaa.gov/paleo/study/26910
Blue Lake	SA	-37.01	140.01	24	Diatom	ecological assemblage, trace	I/E, Temperature	Gouramanis et al. (2010a, 2010b)	45	https://www.ncdc.noaa.gov/paleo/study/22411

						elements, $\delta^{18}O$, $\delta^{13}C$				
Lake Keilambete	VIC	-38.21	142.88	120	Sediment; Ostracods	grain size; geochemistry	I/E	Wilkins et al. (2013a); Wilkins et al. (2013b)	50	https://www.ncdc.noaa.gov/paleo/study/22430
Lake Surprise	VIC	-38.06	141.92	93	Diatoms	ecological assemblage	I/E	Barr et al. (2014a); Barr et al. (2014b)	4	https://www.ncdc.noaa.gov/paleo/study/22432
Lake Elingamite	VIC	-38.35	143.00	121	Diatoms	ecological assemblage	I/E	Barr et al. (2014a); Barr et al. (2014b)	5	https://www.ncdc.noaa.gov/paleo/study/22432
Rebecca Lagoon	TAS	-41.18	144.68	8	Sediment	reflectance	Precipitation	Saunders et al. (2012a); Saunders et al. (2012b)	12	https://www.ncdc.noaa.gov/paleo/study/22416
Snowy Mountains	NSW	-36.46	148.30	1940	Dust	concentration, trace elements	Aridity	Marx et al. (2011a); Marx et al. (2011b)	16	https://www.ncdc.noaa.gov/paleo/study/22413
Jacka Lake	VIC	-36.80	141.80	132	Ostracods	geochemistry, ecological assemblage	I/E, Wind strength	Kemp et al. (2012a); Kemp et al. (2012b)	40	https://www.ncdc.noaa.gov/paleo/study/22414

2.2 Age modeling

New age-depth models were created by Dixon et al. (2017) for each dataset using the Bayesian accumulation histories ('BACON') package in the 'R' platform (Blaauw & Christen, 2011; RCoreTeam, 2015). A detailed methodology of age-depth model construction is presented by Dixon et al. (2017). Each of the 10,000 possible time series for each record ensemble was resampled at 50-year intervals (the maximum sample resolution included in this study) and restricted to the period between 1750CE and 950CE. The youngest age of this range, 1750 CE, was chosen to exclude the post-colonial period, known to contain non-climatic environmental disruption by European land use practices (Barr et al., 2014a; Gell et al., 2009; Gouramanis et al., 2010a). The earliest point of this range, 950 CE, is the earliest point in time covered by all eight records (Figure 2).

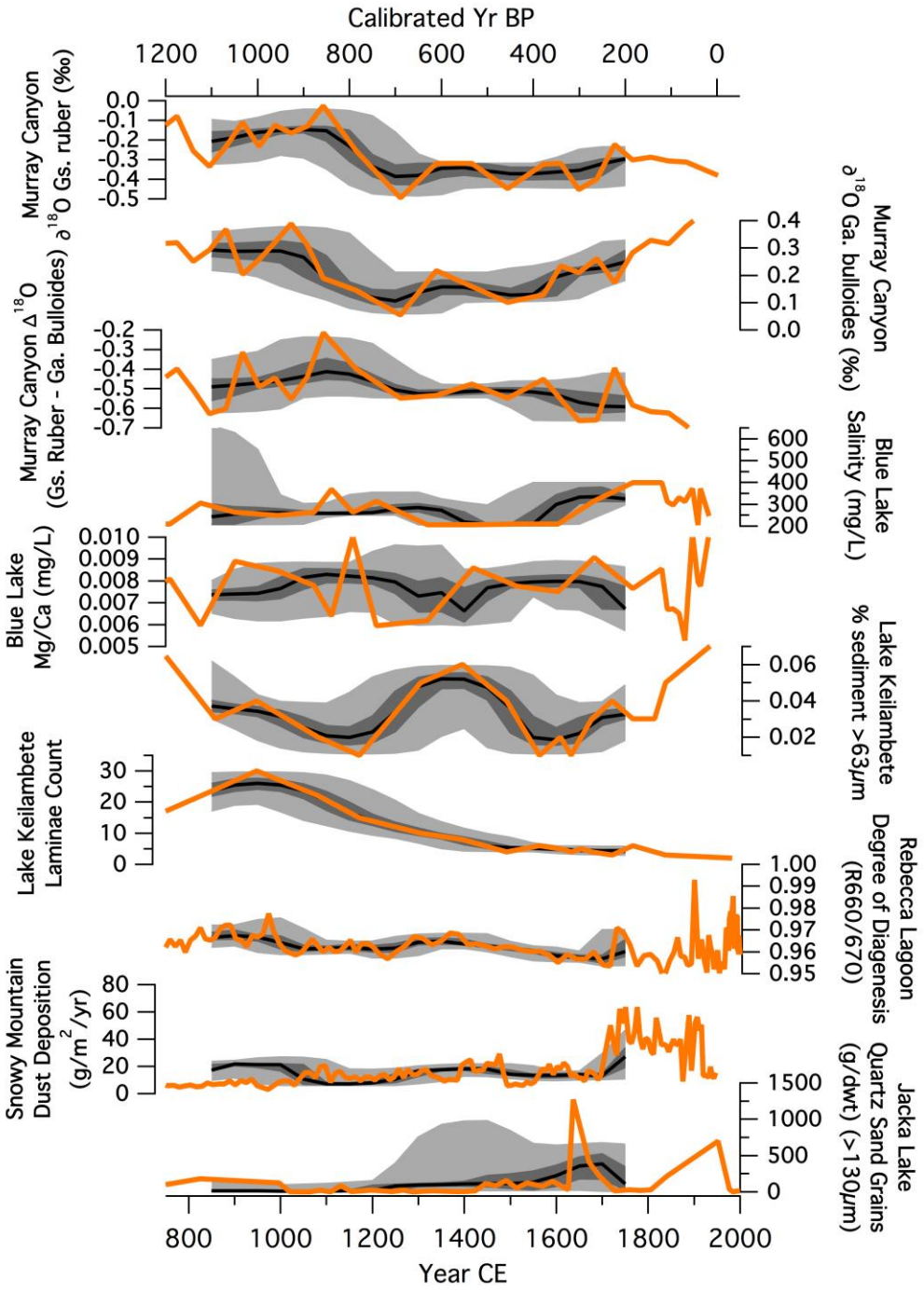

192

193 **Figure 2.** Time-uncertain time series for the hydroclimate sensitive proxies used in this study.
194 The black line and grey shading represent the BACON-derived chronologies; the solid black line
195 is the median timeseries, the dark grey shading represents the 1σ confidence interval, the pale
196 grey shading represents the 2σ confidence interval; the orange line shows the original published
197 timeseries. See table 1 for metadata for sites and proxies.

198 2.3 Site analysis

199 Records from five of the eight southeastern Australia datasets are multivariate in nature
200 (Figure 2), and the remaining three are single-variable records. Here we aim to identify shared
201 climate signals across the suite of measured proxies. Subjective selection of a single proxy
202 within a record may be complicated by doubt about which variable may be representative of the
203 site response. For example, there are X variables at site Y, several of which are likely to be
204 sensitive to hydroclimate. Inclusion of multiple variables from any individual site within a
205 regional synthesis would contradict the assumption of independence of data reduction inputs.
206 The application of data-reduction techniques such as principal component analysis provides an
207 objective means of identifying coherent signals in multivariate paleoclimate records, which can
208 then be assessed for their climate sensitivity and used in regional comparisons (Tierney et al.,
209 2013; Tyler et al., 2015).

210 Principal component analysis (PCA) is the most common method of generating EOFs
211 from paleoclimate data. However, PCA is a linear technique unsuitable for data which exhibit
212 non-linear responses across environmental gradients, as is the case for many biological data for
213 example (Legendre & Legendre, 2012; ter Braak & Juggins, 1993). As a consequence, diatom
214 ecological assemblage data from Lake Surprise and Lake Elingamite were processed using
215 Detrended Correspondence Analysis (DCA) (Hill & Gauch, 1980) to reduce the number of
216 dimensions within the dataset, using the same approach as Tyler et al. (2015). Non-ecological
217 data from Blue Lake, Murray Canyon, and Lake Keilambete were processed using PCA. Both
218 methods were implemented using the 'vegan' package for R (Okansen et al., 2016; RCoreTeam,
219 2015).

220 2.4 Regional analysis

221 The first two EOFs from each multivariate site and the standardized time series from the
222 single-variable sites were incorporated into a common matrix to perform a regional-level, two-
223 tiered PCA analysis ($MCEOF_{TT}$) to explore consistent patterns between all eight sites. Ten
224 thousand iterations of PCA were performed incorporating age modeling uncertainties. The 1σ
225 and 2σ confidence intervals were retained for error estimates. Between iterations, resultant EOFs

have the potential to reverse sign, and this was corrected by multiplying all inverted EOFs by -1 (Anchukaitis & Tierney, 2012; Tyler et al., 2015).

A single-tier regional PCA ($MCEOF_{ST}$) was also carried out with one dataset from each of the eight sites, to investigate whether reduction of multivariate datasets identified climate signals not captured by a single proxy. In this case, the proxy most likely to reflect hydroclimate variability was selected, following the interpretation in the original paper. Each dataset was standardized and resampled as described above.

In order to examine whether one site had a dominating influence on the outcome of the regional data reduction, leave-one-out cross-validation was conducted within the regional $MCEOF_{TT}$, with a different site excluded each time. The significance of the regional EOFs was tested through multiple methods: i) the Kaiser rule, which retains eigenvalues greater than 1 (Kaiser, 1960); ii) the 'broken stick' model which identifies significant EOFs as those which explain more variance than randomly distributed zones within a sequence (Bennett, 1996; Cattell, 1966); and iii) the application of 'rule N' test, which selects EOFs based on whether they explain more variance than an autoregressive red-noise null hypothesis (Anchukaitis & Tierney, 2012; Preisendorfer & Mobley, 1988). The red-noise null hypothesis was based on autoregressive models with parameters set to the sample mean, variance and lag-one autocorrelation of the regional MCEOF: the multivariate site EOFs and the time series from the single-proxy sites. The parameters from the resulting AR models were used to construct 1000 time series with the same mean and standard deviation as the proxy data.

For the purpose of comparing the regional EOFs to existing annually resolved paleoclimate reconstructions, annual records were divided into 50-year bins. Binned datasets were then compared to the EOFs using Pearson correlation coefficients.

3 Results

BACON age-depth models provide interpolated age uncertainties that are not always available in the original datasets (Figure 2). Detailed outcomes of the age modeling, as well as a general discussion of how they differ from the originally published chronologies, is described by Dixon et al. (2017). The PAGES2k selection criteria allowed for the inclusion of records with as few as two dates. A benefit of our method is that it accounts for increased age uncertainty in

255 records with low age density. In particular, some of the re-modeled time series exhibit large
256 uncertainties in part due to chronological uncertainties coupled with the occurrence of large
257 excursions whose mean age falls outside the time period examined here, but which are
258 occasionally incorporated through some age-model iterations. Furthermore, if the timing of these
259 excursions is predicted to occur in a period of large age uncertainties, then the excursion may
260 appear to last longer than in the original age-depth model. Examples of this include Blue Lake
261 and Jacka Lake (Figure 2). Variability in the proxy values in the BACON re-modeled time series
262 is also diminished due to the 50-year binning of the data.

263 Two site-level EOFs were identified for Murray Canyon, Blue Lake, and Lake
264 Keilambete. Outcomes of site-analysis significance tests are discussed in detail in the
265 supplementary information. To maintain an equal number of EOFs from each multivariate site,
266 two EOFs from each site were retained for inclusion in the regional PCA (Figure 3).

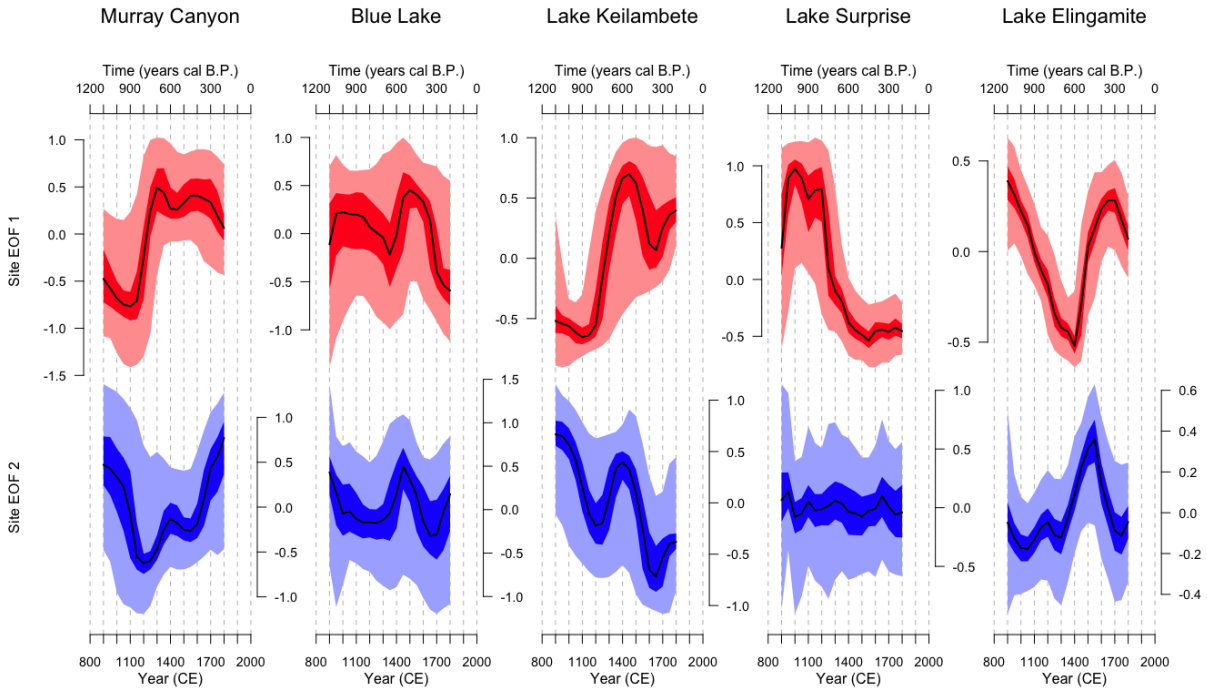

267

268 **Figure 3.** The two leading EOFs resulting from Murray Canyon (PCA; 62% and 38% variance
269 explained, respectively), Blue Lake (PCA; 55% and 45% variance explained, respectively), Lake
270 Keilambete (PCA; 56% and 44% variance explained, respectively), Lake Surprise (DCA), and
271 Lake Elingamite (DCA). Black lines indicate median time series, dark shading represents the 1σ
272 confidence interval, and the pale shading represents the 2σ confidence interval.

The regional $MCEOF_{TT}$ returned two significant patterns of variability (Figure 4), as interpreted through the Kaiser rule and examination of the scree plot. However, the outcome of the 'Rule N' test suggests the first two MCEOFs are significant when compared to the broken stick plot but are not significantly indistinguishable from red noise (Figure 5). The 1σ and 2σ confidence intervals for regional $MCEOF2_{TT}$ do surpass the red-noise level. Leave-one-out bootstrapping indicates that no individual record has a dominant impact on the signal expressed by regional MCEOFs, or the total amount of variance explained by those MCEOFs (Supplementary Figure S2). Other than orientation changes in regional $MCEOF2_{TT}$, the patterns exhibited by the regional MCEOFs remain consistent. When Lake Keilambete or Lake Surprise is excluded, the age uncertainties around regional $MCEOF1_{TT}$ are substantially larger, indicating the importance of these two records in the regional MCEOF analysis.

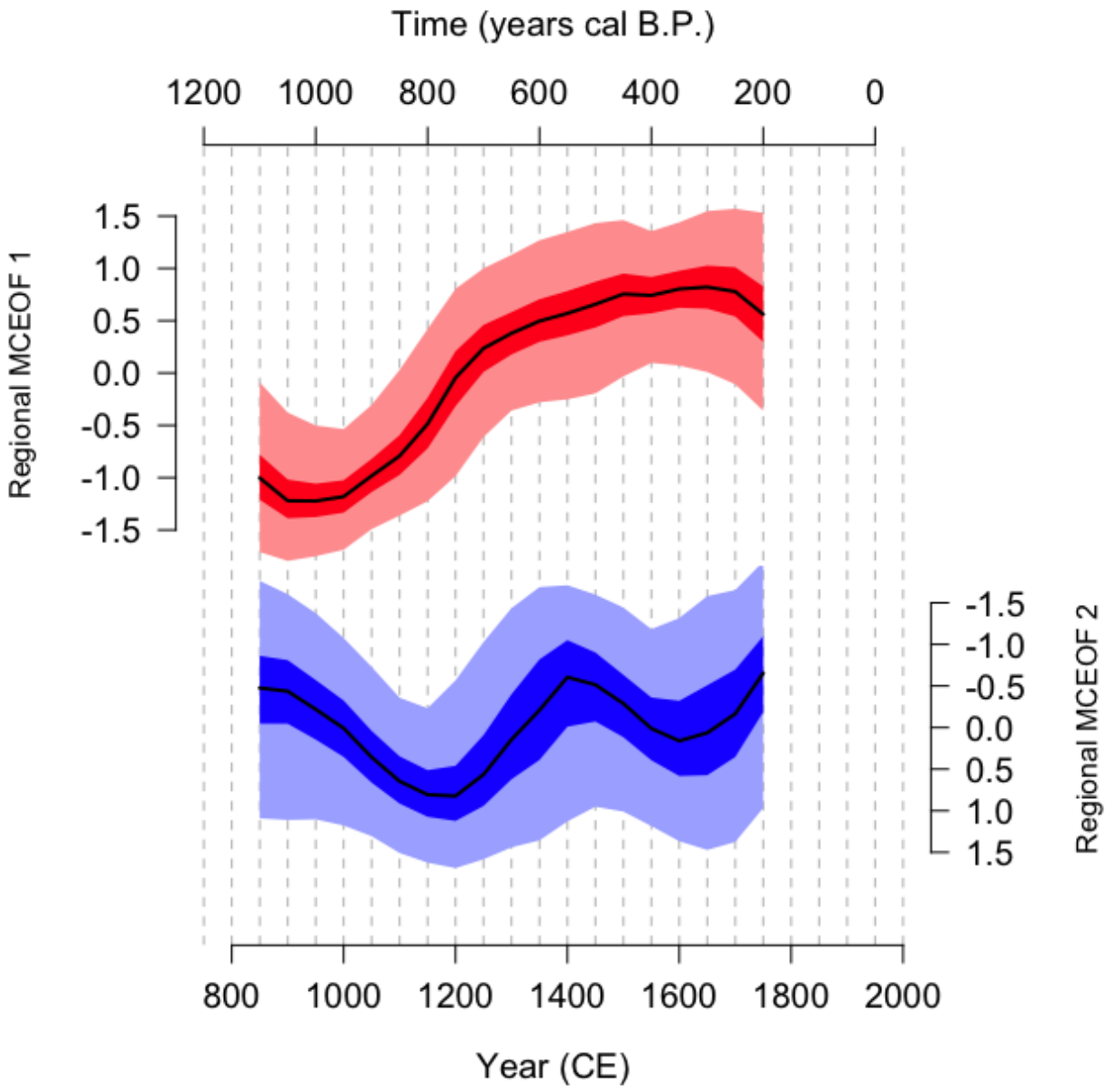

286

287 **Figure 4.** Time series of the two leading regional MCEOFs, resulting from PCA analysis of site-
288 level EOFs and single-proxy time series. Black lines indicate median time series, dark shading
289 represents the 1σ confidence interval, and the pale shading represents the 2σ confidence interval.

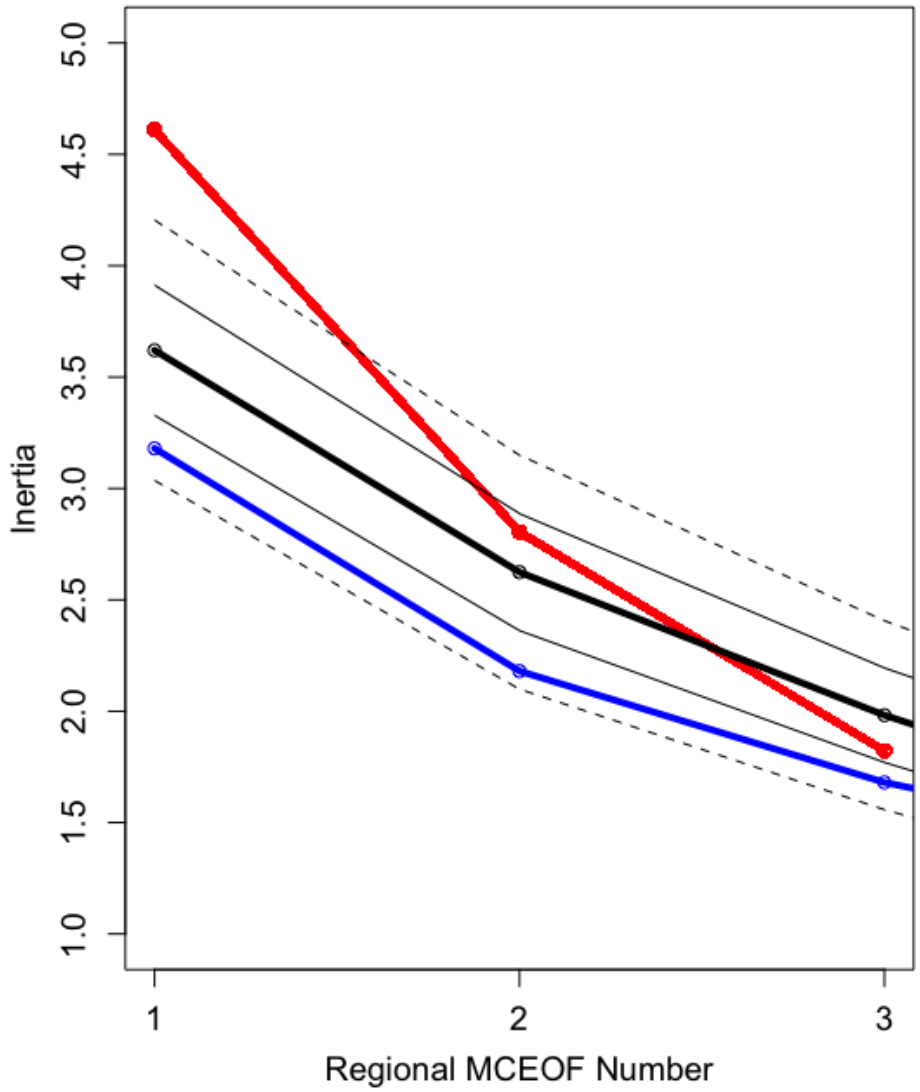

Figure 5. Significance testing of the leading regional MCEOFs. The heavy black line represents the median regional MCEOF outcome, the solid black line and broken black line represent the 1σ and 2σ confidence intervals respectively, the blue line represents the 'broken stick' significance test (Bennett, 1996), and the red line represents the median background red noise Rule N significance test (Anchukaitis & Tierney, 2012).

The pattern expressed by the regional MCEOFs is similar to those seen in the site-level EOFs. Regional MCEOF1$_{TT}$ reaches a minimum at 900CE, and then steadily increases towards a peak between 1750-1800CE. Regional MCEOF2$_{TT}$ displays a bimodal shape, with maxima between 850-1050CE and between 1400-1500CE. Loadings of median multivariate site EOFs and median single-proxy site time series are presented in Figure 6 and Supplementary Figure S3.

The first two regional MCEOFs collectively explain 48.1% of the variance in the regional synthesis: regional MCEOF1$_{TT}$ explains 27.9% and regional MCEOF2$_{TT}$ explains 20.2% of regional variance.

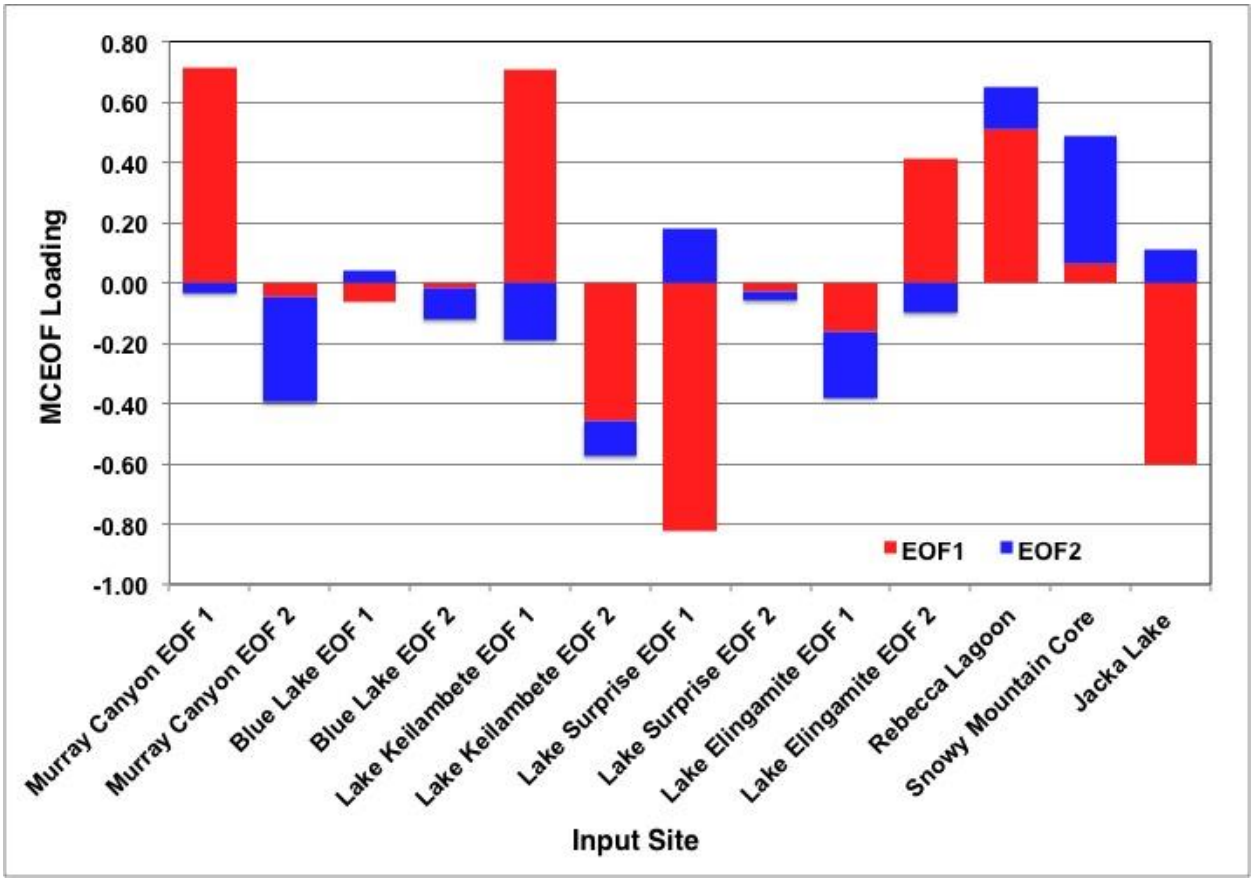

Figure 6. The loadings of each site time series or site EOF on the regional MCEOF outcome (MCEOF1 = red, MCEOF2 = blue).

The MCEOF$_{ST}$ returns principal components somewhat similar to those derived by the two-tier approach. Variance explained is comparable to MCEOF$_{TT}$: regional MCEOF1$_{ST}$ explains 30.4% of variance and regional MCEOF2$_{ST}$ explains 22.1% of variance. However, the regional MCEOF1$_{ST}$ captures patterns seen in MCEOF 1 and 2 in the multi-tiered MCEOF$_{TT}$, and regional MCEOF2$_{ST}$ appears flat and void of any distinct patterns and/or trends. Significance test outcomes for the MCEOF$_{ST}$ indicate that neither MCEOF1$_{ST}$ nor MCEOF2$_{ST}$ are significantly distinguishable from red noise, nor do they pass the broken-stick test (Supplementary Figure S3).

4 Discussion

4.1 Interpretation of site analyses

Each of the site-level EOFs are compared to raw datasets and the published proxy-climate relationship for qualitative interpretation of hydroclimate change within the multivariate datasets. In the Murray Canyon core, two species of foraminifera were analysed by Moros et al. (2009a), each with a different ecological niche. For this reason, it is expected that there are different patterns of variability within the raw data. PCA is performed for this site because stable isotope values are expected to respond in a linear fashion to environmental changes. When the EOFs are compared to the raw time series, it appears that EOF 1 reflects local sea-surface temperature (SST) because of a perfect correlation (r=1.00) between Murray Canyon EOF 1 and *Globigerinoides ruber* $\delta^{18}O$. Murray Canyon EOF 1 correlated very strongly with Lake Keilambete EOF 1 (r=0.87) and Lake Surprise EOF 1 (r=-0.90), and moderately well with Lake Keilambete EOF 2 (r=-0.52) and Lake Elingamite EOF 2 (r=0.55).

Murray Canyon EOF 2 appears to reflect a more regional to hemispheric signal, with a strong relationship between *Globigerina bulloides* and Murray Canyon EOF 2 (r= -0.78) as well as between $\Delta^{18}O$ (*Gs. ruber – Ga. bulloides*) and Murray Canyon EOF 2 (r=0.58). Moros et al. (2009a) interpreted *Ga. bulloides* variability as indicative of El Niño Southern Oscillation (ENSO) activity, centred in the Pacific Ocean, as well as Southern Ocean behaviour during the late Holocene. Based on the published interpretation, it is argued that Murray Canyon EOF 2 is impacted by ENSO behaviour, westerly wind strength, and the intensity of water vapour transport. Murray Canyon EOF 2 displays relatively strong agreement with Blue Lake EOF 1 (r=-0.51) and Lake Elingamite EOF 1 (r=0.66). The published interpretation of the Blue Lake record suggests high variability during the late Holocene but does not propose specific mechanisms. Both ENSO and the Southern Annular Mode (SAM) (the latter indicative of westerly wind strength) are known to impact on the position of the subtropical ridge (Cai et al., 2011), which may lead to a blended signal in palaeoclimate records. Accordingly, Murray Canyon EOF 1 is interpreted as a local signal, while Murray Canyon EOF 2 preserves the larger regional-hemispheric signal.

For the Blue Lake record, geochemical data (Mg/Ca ratios) and reconstructed salinity (mg/L) values were examined using PCA. Blue Lake EOF 1 has a strong relationship with the ostracod-derived salinity reconstruction (r=-0.88), while EOF 2 reflects the ostracod valve Mg/Ca ratios (r=0.92). This strong alignment may indicate that the Mg/Ca does not have a strict salinity/rainfall control and may also reflect the groundwater control on lake levels. Alternatively, the relationship between ostracod Mg/Ca and lake level seen in the instrumental period may not have remained stationary through time. When the Blue Lake EOFs are compared against the interpolated low-resolution $\delta^{18}O$ time series (interpreted to reflect a blend of both I/E ratios and groundwater input to the lake), only moderate correlations are seen with EOF 1 (correlation Blue Lake EOF 1~$\delta^{18}O$: r=-0.41, Blue Lake EOF2~$\delta^{18}O$: r=-0.01). This may be caused by differing response times between variables, resolution disparities, or complications by non-climatic controls. Moderate agreement is displayed between Blue Lake EOF 1 and Murray Canyon EOF 2 (r=-0.51), as well as between Lake Keilambete EOF 2, which is moderately correlated with Blue Lake EOF 2 (r=0.57).

The two hydroclimate-sensitive variables in the Lake Keilambete dataset contribute to both PCA EOFs. Grain size (sediment <63um), traditionally interpreted as a lake-level proxy, has a moderately strong relationship with both EOF 1 (r=-0.59) and EOF 2 (r=-0.63). Previous studies have suggested that the linear relationship between lake levels and I/E disintegrates during times of high lake levels, due to interaction with neighbouring water bodies (Jones et al., 2001; Wilkins et al., 2013b). This has the potential to shift the proxy–climate relationship within the grain-size derived lake-level interpretations. Lamina occurrence, interpreted to have a positive relationship with temperature and precipitation, agrees well with both PC EOF 1 (r=0.87) and EOF 2 (r=-0.70). Original author interpretations indicate a warm/wet period in Lake Keilambete around 950 CE (Wilkins et al., 2013b). Both Lake Keilambete EOF 1 and EOF 2 exhibit a decrease around that time, which suggests a lack of independence between the two variables, despite a low correlation between the raw data (r=0.01). Lake Keilambete EOF 1 correlates strongly with Lake Surprise EOF 1 (r=-0.91) and Murray Canyon EOF 1 (r=0.87), as well as Lake Elingamite EOF 2 (r=0.64), which was interpreted as a hydroclimate signal by Tyler et al. (2015). Lake Keilambete EOF 2 correlates strongly with Murray Canyon EOF 1 (r=-0.52), Blue Lake EOF 2 (r=0.57), and Lake Surprise EOF 1 (r=0.52).

The DCA performed by Tyler et al. (2015) for both Lake Surprise and Lake Elingamite was repeated with the BACON-derived age model instead of the CLAM age model used in that study. The selection of age modelling software has minimal impact on the timing of events, although the BACON age models produce larger age uncertainties. The outcomes from the DCA analysis performed here are nearly identical to the outcomes of Tyler et al. (2015), except for a reversal in sign for DCA EOF 1 for Lake Elingamite. According to Tyler et al. (2015), Lake Elingamite EOF 1 represents shifts in lake depth, as suggested by variations in the dominance of shallow-water benthic/planktonic diatom species versus deep-water planktonic species. Lake Surprise EOF 1 and 2 do not have a clear relationship with the salinity reconstruction, but are controlled by the interplay of ecological niches within the diatom assemblage. Lake Surprise EOF 1 alternates between a positive and negative relation with salinity, depending on the state of Lake Surprise EOF 2. This suggests that there may be some connection with climatic conditions, but not as a dominant driver.

4.2 Single vs. two-tier MCEOF analysis

Previous work has demonstrated the possibility of identifying hydroclimate signals through multi-tiered data reduction techniques in Australian diatom records (Tyler et al., 2015). The present study expands the application of data ordination to analyse a greater diversity of both palaeoclimate archives and proxies measured within these archives. In an effort to assess the value of applying a multi-tier, rather than single-tier, data-reduction approach, a regional PCA of subjectively selected datasets has been carried out alongside. The single-tier regional $MCEOF_{ST}$ returned lower loadings for all sites except Blue Lake and did not pass any of the significance tests (Supplementary Figure S3). This is likely caused by the fewer degrees of freedom present in the regional analysis, which decreases the likelihood of significant result, and is exacerbated by the large uncertainties in the chronologies. The multi-tier approach maintains a greater amount of variance with a larger number of degrees of freedom. The outcomes presented here suggest that the multi-tiered approach is more effective for identifying potential climate patterns that may not be dominant in a qualitatively selected proxy from a multivariate record. However, both $MCEOF_{TT}$ and $MCEOF_{ST}$ exhibit similar patterns.

4.3. Interpretation of regional analysis

The regional synthesis presented in this study identifies common signals among paleoclimate records across southeastern Australia and provides details of the underlying trends within the previously characterised 'unstable' Common Era (Gouramanis et al., 2013; Mooney, 1997; Stanley & De Deckker, 2002). Given that all contributing datasets have been screened for hydroclimate sensitivity, the regional MCEOFs are interpreted to represent patterns of hydroclimate variability. Good agreement between individual sites and regional MCEOFs is evidence for a coherent signal (Figures 3, 4). When the regional MCEOFs are oriented to match the interpretation of the original publications, MCEOF1$_{TT}$ indicates a wetting trend between 900 CE and 1750 CE. Regional MCEOF2$_{TT}$ implies fluctuations between wet and dry conditions, with the wettest periods occurring between 850–950 CE, 1400–1500 CE and 1650–1750 CE (Figure 4). The variance explained by the first two regional MCEOFs (48.1%) is similar to the variance explained in similar studies (Anchukaitis and Tierney 2010 (52% ±10%), Tyler et al., 2015 (48%)). However, the positioning of the regional MCEOF outcomes below the significance level for the rule-N significance tests suggests that non-climatic noise in such a diverse data network may partially obscure climate signals (Figure 5).

Murray Canyon EOF1, Lake Keilambete EOF1, Lake Surprise EOF1, and Rebecca Lagoon, and Jacka Lake load most strongly onto regional MCEOF 1 (Figure 6). Murray Canyon EOF 1 is highly correlated with $\Delta^{18}O$ (*Gs.ruber – Ga. bulloides*) values, which represent water-column stratification as controlled by westerly wind strength (Moros et al., 2009a). Lake Keilambete EOF1 and Lake Keilambete EOF2 correlate well with grain size (<63μm) and laminae occurrence, which respond to precipitation and temperature/precipitation interactions respectively (Wilkins et al., 2013b). The interpretation of Lake Surprise EOF 1 is not clear, but is generally representative of the relative dominance of benthic versus planktonic diatoms, which in turn reflects lake volume changes due to precipitation/evaporation (Tyler et al., 2015). Rebecca Lagoon preserves a precipitation record controlled by westerly wind strength (Saunders et al., 2012a); the Jacka Lake grain-size changes are also associated with precipitation and westerly wind strength (Kemp et al., 2012a). The latitude, proxies, and catchment size of these sites vary, but the influence of the westerly winds, as interpreted by the original authors, is consistent.

Murray Canyon EOF 2, Lake Elingamite EOF 1, and the Snowy Mountain core show strongest loadings onto regional MCEOF2 (Figure 6). The Snowy Mountain site is the most likely to have an appreciable Pacific Ocean influence, given its eastern position and observed influence of Pacific climate modes on Snowy Mountain precipitation (Risbey et al., 2009). Murray Canyon EOF2 is also likely influenced by westerly wind strength and possibly by ENSO-moderated regional water transport (Moros et al., 2009). Regional MCEOF2 peaks at 850–950CE, 1400–1500CE and 1650–1750CE. The timing of these peaks bears some resemblance to periods of increased rainfall in northeast New South Wales, as inferred by a relationship with Antarctic ice-core proxies (Tozer et al., 2018; Tozer et al., 2016; T. Vance et al., 2015), and by centennial resolution or short-duration rainfall reconstructions across western and southern Australia (Cohen et al., 2012; Rouillard et al., 2016; Stanley & De Deckker, 2002; T. Vance et al., 2015). MCEOF2 suggests generally wetter conditions between 1400 and 1750 CE (Figure 4).

One site stands out because of a lack of agreement with the regional patterns: Blue Lake at Mt. Gambier. The EOFs for this record exhibit very low correlation with either of the regional MCEOFs (Figure 6) and exclusion of this record has little impact on the regional MCEOFs (Supplementary Figure S2). Inclusion of the salinity reconstruction in the single-tier regional PCA returns a slightly higher site loading (-0.24), but the low agreement in both approaches suggests that either the chronological uncertainties inhibit precise correlation with the other records or that the salinity or geochemical variability at Blue Lake exhibits a lesser, or time-lagged sensitivity relative to other sites in this synthesis. Blue Lake is heavily influenced by groundwater flow, and lake-groundwater interactions may explain this lack of coherence with the other records. Gouramanis et al. (2010a) suggest that groundwater influence at Blue Lake increases during times of lower precipitation, thus buffering the lake against dramatic shifts in salinity and muting potential climatic I/E signals.

4.4 Drivers of hydroclimate variability in southeastern Australia during the Common Era

Previous studies have suggested that the Common Era was characterized by variable and unstable conditions across southeastern Australia, including effective moisture and temperature anomalies (Cook et al., 2000; Gouramanis et al., 2013; Stanley & De Deckker, 2002). ENSO variability is the most commonly cited driver for late Holocene instability (Bowler, 1981; Cobb et al., 2013; D'Costa et al., 1989; Kemp et al., 2012a; Saunders et al., 2012a). However, the role

460 of the westerly wind belt in driving precipitation trends over recent decades in southern Australia
461 has been highlighted (Hendon et al., 2007; Risbey et al., 2009). Enhanced westerly wind strength
462 and increased storminess since ~350 CE, punctuated by short periods of lessened activity, is
463 indicated by aeolian quartz grain-size analysis at Blue Lake, New South Wales (Stanley & De
464 Deckker, 2002). Increased westerly wind strength on the Australian continent most likely
465 indicates a more negative SAM mean state. A negative trend in SAM between 1CE and
466 ~1480CE supports this interpretation, but SAM values have shifted rapidly toward positive
467 values in the latter half of the last millennium (Abram et al., 2014; Dätwyler et al., 2017). Local
468 sea-surface temperatures (SSTs) in the southern Pacific and Indian Oceans and in the Australian
469 sector of the Southern Ocean declined during the late Holocene (Calvo et al., 2007; Gouramanis
470 et al., 2013; Moros et al., 2009a), which could lead to decreases in effective moisture through
471 suppressed marine evaporation. Terrestrial surface temperatures agree with a negative trend, but
472 also allow for examination of higher-frequency variability: Cook et al., (2000) found reduced
473 temperature variability between 100-1900 CE, and statistical reconstructions suggest a cooling
474 trend between 1350 CE and ~1900 CE punctuated by MCA and LIA-like anomalies (Gergis et
475 al., 2016).

476 Comparison of the outcome of this study with pre-existing palaeoclimate reconstructions
477 allows for both the interpretation of the regional MCEOFs as well as investigation of the
478 preservation of low frequencies in low-resolution palaeoclimate syntheses. The two regional
479 MCEOFs show agreement with existing palaeoclimate reconstructions from both Australia and
480 wider areas (Figure 7). Regional MCEOF1$_{TT}$ suggests an increase in effective moisture in
481 southeastern Australia between 950 CE and 1750 CE, in agreement with the original
482 interpretations of most of the contributing datasets (Barr, 2012; Saunders et al., 2012a; Wilkins
483 et al., 2013b), as well as 19th century lake level highstands observed by early European colonists
484 in the region (Jones et al., 1998; Tibby et al., 2018). When multi-millennial tree ring records in
485 Tasmania and synthesized high-resolution tree ring, ice core, and coral records are compared to
486 the outcomes of this synthesis, similar low-frequency trends are evident (Figure 7). However, the
487 multidecadal signal in the higher resolution records is attenuated in comparison with the signal in
488 the lower resolution archives. This supports the use of low-resolution records for capturing low
489 frequency behavior that may be lost in the high-resolution records.

The effect of temperature on global hydroclimate variability represents one of the most important, yet poorly constrained aspects of future climate change (Berg et al., 2015; Rehfeld & Laepple, 2016). Warming (cooling) may have both positive and negative effects on land surface effective moisture. For example, warmer (cooler) sea-surface and near-surface temperatures encourage increased (decreased) convective evaporation and an increased (decreased) atmospheric water vapor capacity (Wentz & Schabel, 2000). Conversely, warm (cool) land surface temperatures lead to increased (decreased) surface evaporation, which impacts on local effective moisture. Warmer temperatures and low rainfall are often coupled, especially in the form of heatwave and drought conditions (Nicholls & Della-Marta, 2004). However, modelling experiments highlight the importance of atmosphere – soil connections, where sunny conditions with decreased cloud cover can lead to soil-moisture deficits, decreased evaporative cooling, and higher terrestrial surface temperature (Berg et al., 2015; Trenberth & Shea, 2005).

4.4.1 Temperature

In order to identify the potential impact of terrestrial surface temperature on hydroclimate variability in southeastern Australia, the regional MCEOFs were compared to temperature reconstructions from the Mt. Read tree-ring record, Tasmania (Cook et al., 2000; Cook et al., 2006), and the Aus2k multi-proxy synthesis (Gergis et al., 2016). The Mount Read tree-ring record from Tasmania reconstructs warm season (November – April) temperature from Huon pine for the period between 1600 BCE and 2001 CE (Cook et al., 2000; Cook et al., 2006). The warmest period in Tasmania before the onset of the industrial period occurred between 900–1500 CE, which agrees with a period of increasing effective moisture in regional MCEOF1 (Figure 7). However, rather than a distinct LIA temperature anomaly, the period between 1500–1900 CE was characterized by muted multi-decadal variability at Mt. Read (Cook et al., 2000; Cook et al., 2006). Multiple reconstruction techniques applied to the Aus2k network of temperature proxies by Gergis et al. (2016) supported an extended LIA-like cool period between ~1500 – 1900 CE. The same reconstruction suggested that the warmest pre-industrial period occurred between 1150–1350 CE, which also corresponds with the period of lowest effective moisture according to regional MCEOF1 (Figure 7). When Aus2k temperature anomalies were binned to 50-year intervals and compared to regional $MCEOF1_{TT}$, the principal regression analysis, ‘composite plus scale’, and pairwise comparison method approaches showed the strongest agreement (r = -

0.35; -0.36; 0.32), and the Bayesian hierarchical model showed weaker correlation (r = -0.20), despite the low number of overlapping bins (n=17). This agreement between regional $MCEOF1_{TT}$ and the Aus2k temperature record suggests that terrestrial surface temperatures have a negative relationship with regional effective moisture. Warmer air temperatures correspond with increased evaporation from the land surface and lower I/E ratios, while lower air temperatures dampen site-level evaporation and increased I/E ratios, noting that this summary does not include land-surface feedbacks or the effect of changes to variability.

4.4.2 Ocean-atmosphere interactions

On longer time scales, the Tasmanian tree ring-derived surface-temperature reconstruction has a positive correlation with sea-surface temperatures in the southern Indian Ocean and Tasman Sea (Cook et al., 2006). Alkenone-derived local SSTs in the Great Australian Bight suggest cooling over the last 2000 years caused decreased heat export from the Indo-Pacific Warm Pool, punctuated by warmer anomalies during the Medieval Climate Anomaly (650 CE – 950 CE) (Perner et al., 2018). This agrees with the Mount Read temperature reconstruction (Figure 7) and supports the hypothesis that cool conditions occurred across the region during the LIA. Cool SSTs would suppress the potential for evaporation over the oceans and decrease the potential moisture capacity of the lower atmosphere (Wentz & Schabel, 2000). A concurrent increase in effective moisture could be driven by suppressed evaporation driven by cooler temperatures in summer, and/or a shift towards increased winter precipitation in southern Australia. Reconstructions of cool versus warm season rainfall in two sub-regions of southeastern Australia (the Murray Darling Basin and the Southern Slopes (Figure 1 by (Freund et al., 2017) allow for the examination of seasonal shifts. Winter rainfall in the Murray Darling Basin was higher during the LIA than in recent centuries (Figure 7). This suggests that increased effective moisture displayed by MCEOF1 during the LIA is caused by increased winter rainfall, which is less likely to be evaporated.

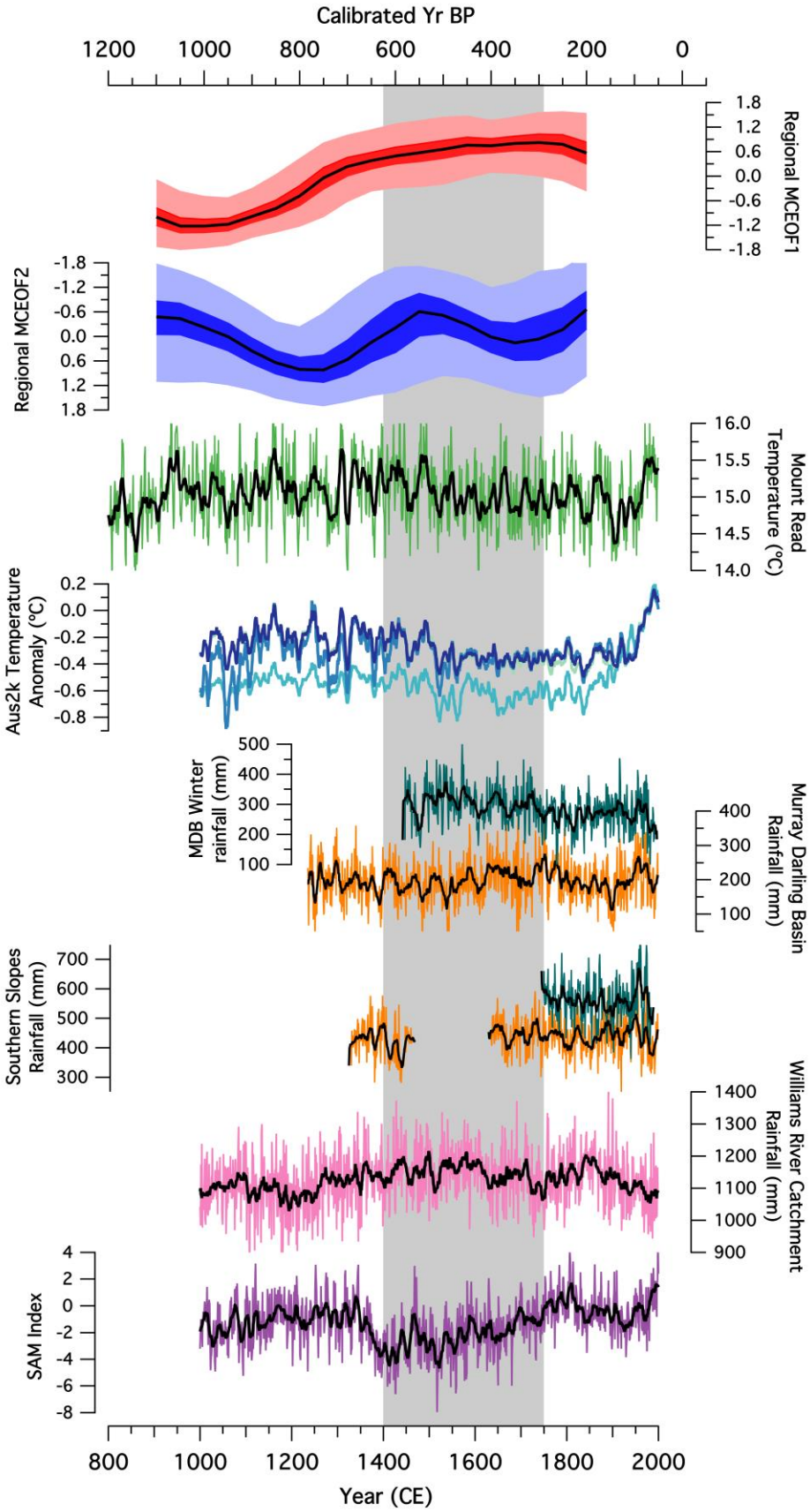
Calibrated Yr BP
1200
1000
800
600
400
200
0
Regional MCEOF1
1.8
1.2
0.6
0.0
-0.6
-1.2
-1.8
Regional MCEOF2
Mount Read Temperature (°C)
16.0
15.5
15.0
14.5
14.0
Aus2k Temperature Anomaly (°C)
0.2
0.0
-0.2
-0.4
-0.6
-0.8
MDB Winter rainfall (mm)
500
400
300
200
100
Murray Darling Basin Rainfall (mm)
Southern Slopes Rainfall (mm)
700
600
500
400
300
Williams River Catchment Rainfall (mm)
1400
1300
1200
1100
1000
900
SAM Index
4
2
0
-2
-4
-6
-8
800
1000
1200
1400
1600
1800
2000
Year (CE)

545

Figure 7. Comparison of (a.) regional EOF1 and (b.) regional EOF2 with Australasian paleoclimate reconstructions: (c.) the Mount Read tree ring-derived temperature reconstruction (Cook et al., 2000; Cook et al., 2006); (d.) the Aus2k temperature reconstructions (Gergis et al., 2016); warm (orange) and cool (green) season rainfall reconstructions for (e.) the Murray Darling Basin and (f.) the southern slopes of Victoria (Freund et al., 2017), (g.) the Williams River catchment rainfall reconstruction (Tozer et al., 2016); (h.) SAM reconstruction from Antarctic proxy records (Abram et al., 2014).

Negative SAM conditions between 1400–1600 CE has been suggested by independent reconstructions (Abram et al., 2014; Dätwyler et al., 2017)(Figure 7), and would likely increase winter rainfall in southern Australia (Power et al., 2006; Risbey et al., 2009). A transition into an El Niño mean state/negative SAM pairing at ~1300 CE has been suggested by Goodwin et al. (2013). Paired negative SAM/El Niño conditions would support an equatorward displacement and overall strengthening of the subtropical ridge (Cai et al., 2011; Drosdowsky, 2005), which reinforces a dominant Southern Ocean influence over southeastern Australia in the period between 1400–1600 CE. Strongly negative values of the SAM index during the LIA support increased winter precipitation at these sites, and highlight the importance of the strength and position of the westerly wind belt for controlling effective moisture in southern Australia during the last 1200 years.

5 Conclusions

Non-annually resolved records of past climate change offer significant potential for deciphering patterns of regional climate variability through the Common Era; however, their utility is often undermined by poor, or inconsistent, chronological control and resolution. Some of these limitations can be addressed by applying a consistent age modelling methodology and accounting for age uncertainties when incorporating paleoclimate data into regional syntheses, in particular using Monte Carlo Empirical Orthogonal Function (MCEOF) analysis (Anchukaitis & Tierney, 2012; Tyler et al., 2015). This study applied a multi-tiered MCEOF to a diversity of paleoclimate archives and proxies from southeastern Australia in order to examine common trends in records. Regional MCEOFs identify common patterns of variability within and between sites (n=8) in southeastern Australia. The results of this study support previous findings of a variable hydroclimate during the Common Era; however, an overarching increase in effective

moisture between 800 CE and 1700 CE is the dominant pattern of variability in the majority of southeastern Australian records. The significance of the regional modes varies between significance testing techniques, and problems persist due to generally poor constraints on sediment age and sampling resolution, despite the application of internationally accepted data selection criteria. Further efforts are required to address the need for more, higher quality records of hydroclimate variability across Australia. However, the change in effective moisture identified by regional MCEOF analysis is robust beyond the age uncertainties and represents a tangible pattern of variability in southeastern Australia that can be tested in future research.

Together, the regional MCEOFs support a wet, cool Little Ice Age in southeastern Australia relative to average conditions during the last 1200 years. Although cooler summer land-surface temperatures may explain some of this pattern, changes in the seasonality of rainfall driven by atmospheric circulation changes and Southern Ocean versus Pacific Ocean based climate modes may be a factor behind this trend. The regional MCEOFs display similar low-frequency trends to those shown in temperature and rainfall reconstructions from remote tree ring, coral, and ice core data. This suggests that continuous, multi-decadally resolved records retain similar signals to annually resolved data when records are compared at a common time scale. Overall, this study demonstrates that multi-tiered EOFs are a useful way to synthesize multivariate and single proxy sedimentary datasets in a data-sparse region. Future efforts will continue to understand, model, and calibrate proxy records for use in quantitative climate reconstructions.

Acknowledgments, Samples, and Data

- The authors declare that they have no conflict of interest.
- Original datasets used in this study can be obtained from the URLs listed in table 1. The recalibrated BACON age models used in the EOFs can be obtained from the NOAA paleoclimate archive (ftp://ftp.ncdc.noaa.gov/pub/data/paleo/pages2k/dixon2017australasia/, NOAA, 2017)
- This work was undertaken while BCD was the recipient of an Australian Post-Graduate Award and an Australian Institute of Nuclear Science and Engineering (AINSE) post-graduate research award.

- The authors wish to thank the original datasets creators, Joelle Gergis for her guidance in the Aus2k working group, and Frederick Michna for creating the map used in this paper.

References

Abram, N. J., Mulvaney, R., Vimeux, F., Phipps, S. J., Turner, J., & England, M. H. (2014). Evolution of the Southern Annular Mode during the past millennium. *Nature Clim. Change, 4*(7), 564-569. Letter. http://dx.doi.org/10.1038/nclimate2235

Allen, K. J., Nichols, S. C., Evans, R., Allie, S., Carson, G., Ling, F., et al. (2017). A 277 year cool season dam inflow reconstruction for Tasmania, southeastern Australia. *Water Resources Research, 53*(1), 400-414. Article.

Allen, K. J., Nichols, S. C., Evans, R., Cook, E. R., Allie, S., Carson, G., et al. (2015). Preliminary December-January inflow and streamflow reconstructions from tree rings for western Tasmania, southeastern Australia. *Water Resources Research, 51*(7), 5487-5503. Article.

Anchukaitis, K. J., & Tierney, J. E. (2012). Identifying coherent spatiotemporal modes in time-uncertain proxy paleoclimate records. *Climate Dynamics, 41*(5-6), 1291-1306. http://dx.doi.org/10.1007/s00382-012-1483-0

Andreu, L., Gutierrez, E., Macias, M., Ribas, M., Bosch, O., & Camarero, J. J. (2007). Climate increases regional tree-growth variability in Iberian pine forests. *Global Change Biology, 13*(4), 804-815. Article.

Ansell, T. J., Reason, C. J. C., Smith, I. N., & Keay, K. (2000). Evidence for decadal variability in southern Australian rainfall and relationships with regional pressure and sea surface temperature. *International Journal of Climatology, 20*(10), 1113-1129. Article.

Ashcroft, L., Karoly, D. J., & Gergis, J. (2014). Southeastern Australian climate variability 1860-2009: a multivariate analysis. *International Journal of Climatology, 34*(6), 1928-1944. Article.

Ashok, K., Guan, Z. Y., & Yamagata, T. (2003). Influence of the Indian Ocean Dipole on the Australian winter rainfall. *Geophysical Research Letters, 30*(15).

Barr, C. (2012). A fine-resolution reconstruction of climatic variability in southeastern Australia over the last 1500 years. *Quaternary International, 279–280*(0), 40.

Barr, C., Tibby, J., Gell, P., Tyler, J., Zawadzki, A., & Jacobsen, G. E. (2014a). Climate variability in south-eastern Australia over the last 1500 years inferred from the high-resolution diatom records of two crater lakes. *Quaternary Science Reviews, 95*(0), 115-131.

Barr, C., Tibby, J., Gell, P., Tyler, J. J., Zawadzki, A., & Jacobson, G. E. (2014b). *Southeast Australia 1500 year crater lake salinity reconstructions*. Retrieved from: https://www.ncdc.noaa.gov/paleo/study/22432

Battarbee, R. W. (2000). Palaeolimnological approaches to climate change, with special regard to the biological record. *Quaternary Science Reviews, 19*(1-5), 107-124. Article; Proceedings Paper.

Bellenger, H., Guilyardi, E., Leloup, J., Lengaigne, M., & Vialard, J. (2014). ENSO representation in climate models: from CMIP3 to CMIP5. *Climate Dynamics, 42*(7-8), 1999-2018. Article.

Bennett, K. D. (1996). Determination of the number of zones in a biostratigraphical sequence. *New Phytologist, 132*(1), 155-170. Article.

Berg, A., Lintner, B. R., Findell, K., Seneviratne, S. I., van den Hurk, B., Ducharne, A., et al. (2015). Interannual Coupling between Summertime Surface Temperature and Precipitation over Land: Processes and Implications for Climate Change. *Journal of Climate, 28*(3), 1308-1328. Article.

Blaauw, M., & Christen, J. A. (2011). Flexible Paleoclimate Age-Depth Models Using an Autoregressive Gamma Process. *Bayesian Analysis, 6*(3), 457-474. Article.

Bowler, J. M. (1981). Australian salt lakes - a paleohydrologic approach. *Hydrobiologia, 81-2*(JUN), 431-444. Article.

Buckley, B., Ogden, J., Palmer, J., Fowler, A., & Salinger, J. (2000). Dendroclimatic interpretation of tree-rings in Agathis australis (kauri). 1. Climate correlation functions and master chronology. *Journal of the Royal Society of New Zealand, 30*(3), 263-276. Article.

Cai, W. J., Purich, A., Cowan, T., van Rensch, P., & Weller, E. (2014). Did Climate Change-Induced Rainfall Trends Contribute to the Australian Millennium Drought? *Journal of Climate, 27*(9), 3145-3168. Article.

Cai, W. J., van Rensch, P., & Cowan, T. (2011). Influence of Global-Scale Variability on the Subtropical Ridge over Southeast Australia. *Journal of Climate, 24*(23), 6035-6053. Article.

Calvo, E., Pelejero, C., De Deckker, P., & Logan, G. A. (2007). Antarctic deglacial pattern in a 30 kyr record of sea surface temperature offshore South Australia. *Geophysical Research Letters, 34*(13). Article.

Cattell, R. B. (1966). Scree test for number of factors. *Multivariate Behavioral Research, 1*(2), 245-276. Article.

Clark, P. U., Hostetler, S. W., Pisias, N. G., Schmittner, A., & Meissner, K. J. (2007). Mechanism for an ~7-kya climate and sea level oscillation during marine isotope stage #. In *Ocean circulation: mechanisms and impacts* (pp. 209-246): American Geophysical Union.

Cobb, K. M., Westphal, N., Sayani, H. R., Watson, J. T., Di Lorenzo, E., Cheng, H., et al. (2013). Highly Variable El Nino-Southern Oscillation Throughout the Holocene. *Science, 339*(6115), 67-70. Article.

Cohen, T. J., Nanson, G. C., Jansen, J. D., Gliganic, L. A., May, J. H., Larsen, J. R., et al. (2012). A pluvial episode identified in arid Australia during the Medieval Climatic Anomaly. *Quaternary Science Reviews, 56*, 167-171. Article.

Consortium, P. k., Ahmed, M., Anchukaitis, K. J., Asrat, A., Borgaonkar, H. P., Braida, M., et al. (2013). Continental-scale temperature variability during the past two millennia. *Nature Geoscience, 6*(5), 339-346. Article.

Cook, E. R., Buckley, B. M., D'Arrigo, R. D., & Peterson, M. J. (2000). Warm-season temperatures since 1600 BC reconstructed from Tasmanian tree rings and their relationship to large-scale sea surface temperature anomalies. *Climate Dynamics, 16*(2-3), 79-91. Article.

Cook, E. R., Buckley, B. M., Palmer, J. G., Fenwick, P., Peterson, M. J., Boswijk, G., & Fowler, A. (2006). Millennia-long tree-ring records from Tasmania and New Zealand: a basis for modelling climate variability and forcing, past, present and future. *Journal of Quaternary Science, 21*(7), 689-699. Article.

Cullen, L. E., & Grierson, P. F. (2009). Multi-decadal scale variability in autumn-winter rainfall in south-western Australia since 1655 AD as reconstructed from tree rings of Callitris columellaris. *Climate Dynamics, 33*(2-3), 433-444.

D'Costa, D. M., Edney, P., Kershaw, A. P., & De Deckker, P. (1989). Late Quaternary paleoecology of Tower Hill, Victoria, Australia. *Journal of Biogeography, 16*(5), 461-482. Article.

Dätwyler, C., Neukom, R., Abram, N. J., Gallant, A. J. E., Grosjean, M., Jacques-Coper, M., et al. (2017). Teleconnection stationarity, variability and trends of the Southern Annular Mode (SAM) during the last millennium. *Climate Dynamics*. journal article.

Dixon, B. C., Tyler, J. J., Lorrey, A. M., Goodwin, I., Gergis, J., & Drysdale, R. (2017a). Low-resolution Australasian palaeoclimate records of the last 2000 years. *Climate of the Past, 13*, 1403-1433. https://doi.org/10.5194/cp-13-1403-2017

Dixon, B. C., Tyler, J. J., Lorrey, A. M., Goodwin, I. D., Gergis, J., & Drysdale, R. N. (2017b). *Recalculated age-depth models for Australasian palaeoclimate records of the last 2000 years*. Retrieved from: https://www.ncdc.noaa.gov/paleo/study/21731

Drosdowsky, W. (2005). The latitude of the subtropical ridge over eastern Australia: The L index revisited. *International Journal of Climatology, 25*(10), 1291-1299. Article.

Fairchild, I. J., Smith, C. L., Baker, A., Fuller, L., Spotl, C., Mattey, D., & McDermott, F. (2006). Modification and preservation of environmental signals in speleothems. *Earth-Science Reviews, 75*(1-4), 105-153.

Freund, M., Henley, B. J., Karoly, D. J., Allen, K. J., & Baker, P. J. (2017). Multi-century cool- and warm-season rainfall reconstructions for Australia's major climatic regions. *Clim. Past, 13*(12), 1751-1770. https://www.clim-past.net/13/1751/2017/

Fritz, S. C. (2008). Deciphering climatic history from lake sediments. *Journal of Paleolimnology, 39*(1), 5-16. Review.

Gallant, A. J. E., Kiem, A. S., Verdon-Kidd, D. C., Stone, R. C., & Karoly, D. J. (2011). Understanding climate processes in the Murray-Darling Basin: utility and limitations for natural resources management. *Hydrology & Earth System Sciences Discussions, 8*(4), 7873-7918. Article.

Gell, P., Fluin, J., Tibby, J., Hancock, G., Harrison, J., Zawadzki, A., et al. (2009). Anthropogenic acceleration of sediment accretion in lowland floodplain wetlands, Murray-Darling Basin, Australia. *Geomorphology, 108*(1-2), 122-126. Article.

Gergis, J., Gallant, A. J. E., Braganza, K., Karoly, D. J., Allen, K., Cullen, L., et al. (2012). On the long-term context of the 1997-2009 'Big Dry' in South-Eastern Australia: insights from a 206-year multi-proxy rainfall reconstruction. *Climatic Change, 111*(3-4), 923-944. Article.

Gergis, J., Neukom, R., Gallant, A. J. E., & Karoly, D. J. (2016). Australasian Temperature Reconstructions Spanning the Last Millennium. *Journal of Climate, 29*(15), 5365-5392. http://journals.ametsoc.org/doi/abs/10.1175/JCLI-D-13-00781.1

Gouramanis, C., De Deckker, P., Switzer, A. D., & Wilkins, D. (2013). Cross-continent comparison of high-resolution Holocene climate records from southern Australia - Deciphering the impacts of far-field teleconnections. *Earth-Science Reviews, 121*, 55-72. Article.

Gouramanis, C., Wilkins, D., & De Deckker, P. (2010a). 6000 years of environmental changes recorded in Blue Lake, South Australia, based on ostracod ecology and valve chemistry. *Palaeogeography Palaeoclimatology Palaeoecology, 297*(1), 223-237. Article.

Gouramanis, C., Wilkins, D., & De Deckker, P. (2010b). *Blue Lake, South Australia 6000 year ostracod geochemical data*. Retrieved from: https://www.ncdc.noaa.gov/paleo/study/22411

Grose, M., Abbs, D., Bhend, J., Chiew, F., Church, J., Ekström, M., et al. (2015). *Southern slopes cluster report, Climate change in Australia Projections for Australia's natural resource management regions*. Retrieved from

Hendon, H. H., Thompson, D. W. J., & Wheeler, M. C. (2007). Australian rainfall and surface temperature variations associated with the Southern Hemisphere annular mode. *Journal of Climate, 20*(11), 2452-2467. Article.

Hendy, E. J., Gagan, M. K., Alibert, C. A., McCulloch, M. T., Lough, J. M., & Isdale, P. J. (2002). Abrupt decrease in tropical Pacific Sea surface salinity at end of Little Ice Age. *Science, 295*(5559), 1511-1514. Article.

Henley, B. J., Meehl, G., Power, S. B., Folland, C. K., King, A. D., Brown, J. N., et al. (2017). Spatial and temporal agreement in climate model simulations of the Interdecadal Pacific Oscillation. *Environmental Research Letters, 12*(4), 11. Article.

Henley, B. J., Thyer, M. A., Kuczera, G., & Franks, S. W. (2011). Climate-informed stochastic hydrological modeling: Incorporating decadal-scale variability using paleo data. *Water Resources Research, 47*. Article.

Hill, M. O., & Gauch, H. G. (1980). Detrended Correspondence Analysis - An improved ordination technique. *Vegetatio, 42*(1-3), 47-58. Article.

Jones, R. N., Bowler, J. M., & McMahon, T. A. (1998). A high resolution Holocene records of P/E ratio from closed lakes in Western Victoria. *Paleoclimates, 3*, 51-82.

Jones, R. N., McMahon, T., & Bowler, J. M. (2001). Modelling historical lake levels and recent climate change at three closed lakes, Western Victoria, Australia (c.1840-1990). *Journal of Hydrology, 246*(1-4), 159-180. Article.

Kaiser, H. F. (1960). The application of electronic computers to factor analysis. *Educational and Psychological Measurement, 20*(1), 141-151. Article.

Kemp, J., Radke, L. C., Olley, J., Juggins, S., & De Deckker, P. (2012a). Holocene lake salinity changes in the Wimmera, southeastern Australia, provide evidence for millennial-scale climate variability. *Quaternary Research, 77*(1), 65-76. Article.

Kemp, J., Radke, L. C., Olley, J., Juggins, S., & De Deckker, P. (2012b). *Wimmera Lakes, Australia Holocene ostracod salinity reconstruction*. Retrieved from: https://www.ncdc.noaa.gov/paleo/study/22414

Kiem, A. S., & Franks, S. W. (2004). Multi-decadal variability of drought risk, eastern Australia. *Hydrological Processes, 18*(11), 2039-2050.

Kiem, A. S., Franks, S. W., & Kuczera, G. (2003). Multi-decadal variability of flood risk. *Geophysical Research Letters, 30*(2). Article.

Kiem, A. S., Johnson, F., Westra, S., van Dijk, A., Evans, J. P., O'Donnell, A., et al. (2016). Natural hazards in Australia: droughts. *Climatic Change, 139*(1), 37-54. Article.

Legendre, P., & Legendre, L. F. (2012). *Numerical ecology* (Vol. 24): Elsevier.

Lough, J. M. (2007). Tropical river flow and rainfall reconstructions from coral luminescence: Great Barrier Reef, Australia. *Paleoceanography, 22*(2). Article.

Marx, S. K., Kamber, B. A., McGowan, H. A., & Denholm, J. (2011a). *Upper Snowy Mountains, Australia 6500 year dust deposition data*. Retrieved from: https://www.ncdc.noaa.gov/paleo/study/22413

Marx, S. K., Kamber, B. S., McGowan, H. A., & Denholm, J. (2011b). Holocene dust deposition rates in Australia's Murray-Darling Basin record the interplay between aridity and the position of the mid-latitude westerlies. *Quaternary Science Reviews, 30*(23-24), 3290-3305. Article.

Mason, I. M., Guzkowska, M. A. J., Rapley, C. G., & Streetperrott, F. A. (1994). The response of lake levels and areas to climate change. *Climatic Change, 27*(2), 161-197. Article.

Mooney, S. (1997). A fine-resolution paleoclimatic reconstruction of the last 2000 years, from Lake Keilambete, southeastern Australia. *The Holocene, 7*(2), 139-149. Article.

Moros, M., De Deckker, P., Jansen, E., Perner, K., & Telford, R. J. (2009a). Holocene climate variability in the Southern Ocean recorded in a deep-sea sediment core off South Australia. *Quaternary Science Reviews, 28*(19-20), 1932-1940. Article.

Moros, M., De Deckker, P., Jansen, E., Perner, K., & Telford, R. J. (2009b). *Murray Canyon MD03-2611 Holocene Foraminifera Stable Isotope Data*. Retrieved from: https://www.ncdc.noaa.gov/paleo-search/study/26910

Murphy, B. F., & Timbal, B. (2008). A review of recent climate variability and climate change in southeastern Australia. *International Journal of Climatology, 28*(7), 859-879. Review.

Neukom, R., & Gergis, J. (2012). Southern Hemisphere high-resolution palaeoclimate records of the last 2000 years. *The Holocene, 22*(5), 501-524. Review.

Nicholls, N., & Della-Marta, P. (2004). 20th century changes in temperature and rainfall in New South Wales. *Australian Meteorological Magazine, 53*(4), 263-268. Article.

Okansen, J., Blanchet, F. G., Kindt, R., Legendre, P., Minchin, P. R., O'Hara, R. B., et al. (2016). vegan: Community Ecology Package. Retrieved from http://CRAN.R-project.org/package=vegan

Palmer, J. G., Cook, E. R., Turney, C. S. M., Allen, K., Fenwick, P., Cook, B. I., et al. (2015). Drought variability in the eastern Australia and New Zealand summer drought atlas (ANZDA, CE 1500–2012) modulated by the Interdecadal Pacific Oscillation. *Environmental Research Letters, 10*(12), 124002.

Perner, K., Moros, M., De Deckker, P., Blanz, T., Wacker, L., Telford, R., et al. (2018). Heat export from the tropics drives mid to late Holocene palaeoceanographic changes offshore southern Australia. *Quaternary Science Reviews, 180*, 96-110.

Power, S., Casey, T., Folland, C., Colman, A., & Mehta, V. (1999a). Inter-decadal modulation of the impact of ENSO on Australia. *Climate Dynamics, 15*(5), 319-324. Article.

Power, S., Haylock, M., Colman, R., & Wang, X. D. (2006). The predictability of interdecadal changes in ENSO activity and ENSO teleconnections. *Journal of Climate, 19*(19), 4755-4771. Review.

Power, S., Tseitkin, F., Mehta, V., Lavery, B., Torok, S., & Holbrook, N. (1999b). Decadal climate variability in Australia during the twentieth century. *International Journal of Climatology, 19*(2), 169-184.

Preisendorfer, R. W., & Mobley, C. D. (1988). *Principal component analysis in meteorology and oceanography* (Vol. 425): Elsevier Amsterdam.

RCoreTeam. (2015). R: A language and environment for statistical computing. Vienna, Australia: R Foundation for Statistical Computing. Retrieved from http://www.R-project.org

Rehfeld, K., & Laepple, T. (2016). Warmer and wetter or warmer and dryer? Observed versus simulated covariability of Holocene temperature and rainfall in Asia. *Earth and Planetary Science Letters, 436*, 1-9. Article.

Risbey, J. S., Pook, M. J., McIntosh, P. C., Wheeler, M. C., & Hendon, H. H. (2009). On the Remote Drivers of Rainfall Variability in Australia. *Monthly Weather Review, 137*(10), 3233-3253. Article.

Rouillard, A., Skrzypek, G., Turney, C., Dogramaci, S., Hua, Q., Zawadzki, A., et al. (2016). Evidence for extreme floods in arid subtropical northwest Australia during the Little Ice Age chronozone (CE 1400–1850). *Quaternary Science Reviews, 144*, 107-122.

Saunders, K. M., Kamenik, C., Hodgson, D. A., Hunziker, S., Siffert, L., Fischer, D., et al. (2012a). Late Holocene changes in precipitation in northwest Tasmania and their potential links to shifts in the Southern Hemisphere westerly winds. *Global and Planetary Change, 92-93*, 82-91. Article.

Saunders, K. M., Kamenik, C., Hodgson, D. A., Hunziker, S., Siffert, L., Fischer, D., et al. (2012b). *Rebecca Lagoon, Tasmania 3700 year sediment reflectance and precipitation reconstruction*. Retrieved from: https://www.ncdc.noaa.gov/paleo/study/22416

Shakun, J. D., & Carlson, A. E. (2010). A global perspective on Last Glacial Maximum to Holocene climate change. *Quaternary Science Reviews, 29*(15-16), 1801-1816. Article.

Speer, M. S., Leslie, L. M., & Fierro, A. O. (2011). Australian east coast rainfall decline related to large scale climate drivers. *Climate Dynamics, 36*(7-8), 1419-1429. Article.

Stanley, S., & De Deckker, P. (2002). A Holocene record of allochthonous, aeolian mineral grains in an Australian alpine lake; implications for the history of climate change in southeastern Australia. *Journal of Paleolimnology, 27*(2), 207-219. Article.

Taschetto, A. S., & England, M. H. (2009). An analysis of late twentieth century trends in Australian rainfall. *International Journal of Climatology, 29*(6), 791-807. Article.

ter Braak, C. J. F., & Juggins, S. (1993). Weighted averaging partial least-squares regression (WA-PLS) - An improved method for reconstructing environmental variables from species assemblages. *Hydrobiologia, 269*, 485-502. Article.

Tibby, J., Tyler, J. J., & Barr, C. (2018). Post little ice age drying of eastern Australia conflates understanding of early settlement impacts. *Quaternary Science Reviews*. http://www.sciencedirect.com/science/article/pii/S0277379118302051

Tierney, J. E., Smerdon, J. E., Anchukaitis, K. J., & Seager, R. (2013). Multidecadal variability in East African hydroclimate controlled by the Indian Ocean. *Nature, 493*(7432), 389-392. Article.

Tozer, C. R., Kiem, A. S., Vance, T. R., Roberts, J. L., Curran, M. A. J., & Moy, A. D. (2018). Reconstructing pre-instrumental streamflow in Eastern Australia using a water balance approach. *Journal of Hydrology, 558*, 632-646.

Tozer, C. R., Vance, T. R., Roberts, J. L., Kiem, A. S., Curran, M. A. J., & Moy, A. D. (2016). An ice core derived 1013-year catchment-scale annual rainfall reconstruction in subtropical eastern Australia. *Hydrology and Earth System Sciences, 20*(5), 1703-1717. Article.

Treble, P., Shelley, J. M. G., & Chappell, J. (2003). Comparison of high resolution sub-annual records of trace elements in a modern (1911-1992) speleothem with instrumental climate data from southwest Australia. *Earth and Planetary Science Letters, 216*(1-2), 141-153. Article.

Trenberth, K. E., & Shea, D. J. (2005). Relationships between precipitation and surface temperature. *Geophysical Research Letters, 32*(14), 4. Article.

Tyler, J. J., Mills, K., Barr, C., Sniderman, J. M. K., Gell, P. A., & Karoly, D. J. (2015). Identifying coherent patterns of environmental change between multiple, multivariate records: an application to four 1000-year diatom records from Victoria, Australia. *Quaternary Science Reviews, 119*(0), 94-105.

van Dijk, A., Beck, H. E., Crosbie, R. S., de Jeu, R. A. M., Liu, Y. Y., Podger, G. M., et al. (2013). The Millennium Drought in southeast Australia (2001-2009): Natural and human causes and implications for water resources, ecosystems, economy, and society. *Water Resources Research, 49*(2), 1040-1057. Article.

van Ommen, T. D., & Morgan, V. (2010). Snowfall increase in coastal East Antarctica linked with southwest Western Australian drought. *Nature Geoscience, 3*(4), 267-272. Article.

Vance, T., Roberts, J., Plummer, C., Kiem, A., & Van Ommen, T. (2015). Interdecadal Pacific variability and eastern Australian megadroughts over the last millennium. *Geophysical Research Letters, 42*(1), 129-137.

Vance, T. R., van Ommen, T. D., Curran, M. A. J., Plummer, C. T., & Moy, A. D. (2013). A Millennial Proxy Record of ENSO and Eastern Australian Rainfall from the Law Dome Ice Core, East Antarctica. *Journal of Climate, 26*(3), 710-725. Article.

Weller, E., & Cai, W. J. (2013). Realism of the Indian Ocean Dipole in CMIP5 Models: The Implications for Climate Projections. *Journal of Climate, 26*(17), 6649-6659. Article.

Wentz, F. J., & Schabel, M. (2000). Precise climate monitoring using complementary satellite data sets. *Nature, 403*(6768), 414-416. Article.

Wigdahl, C. R., Saros, J. E., Fritz, S. C., Stone, J. R., & Engstrom, D. R. (2014). The influence of basin morphometry on the regional coherence of patterns of diatom-inferred salinity in lakes of the northern Great Plains (USA). *The Holocene, 24*(5), 603-613. Article.

Wilkins, D., De Deckker, P., Fifield, L. K., Gouramanis, C., & Olley, J. (2013a). *Lake Keilambete, SE Australia Holocene sediment data and lake level*. Retrieved from: https://www.ncdc.noaa.gov/paleo/study/22430

Wilkins, D., Gouramanis, C., De Deckker, P., Fifield, L. K., & Olley, J. (2013b). Holocene lake-level fluctuations in Lakes Keilambete and Gnotuk, southwestern Victoria, Australia. *The Holocene, 23*(6), 784-795. Article.

Zheng, F., Li, J. P., Clark, R. T., & Nnamchi, H. C. (2013). Simulation and Projection of the Southern Hemisphere Annular Mode in CMIP5 Models. *Journal of Climate, 26*(24), 9860-9879. Article.